



Sudan University of Science and Technology
College of Petroleum Engineering & Technology
Petroleum Engineering Department



**Experimental Investigation Of Seismic Stimulation
Recovery As Case Study In Heglig Area**

**تجربة أثار الإهتزازات السيزمية في إستخلاص النفط
(حقل هجليج منطقة الدراسة)**

*This dissertation is submitted as a partial requirement of B-tech degree
(honor) in petroleum engineering*

Prepared by:

- Abubaker Eltayeb Musaad
- Hesham Mohamed Saeed Alddo
- Khalid Abd Albagi Alamin
- Mohamed Mohamed Almutasim Babiker

Supervisor:

Dr. Alradi Abass Mohamed

October 2016

إِسْتِهْلَالٌ

بِسْمِ اللَّهِ الرَّحْمَنِ الرَّحِيمِ

(فَتَعَالَى اللَّهُ الْمَلِكُ الْحَقُّ وَكَأْتَعْجَلُ بِالْقُرْآنِ مِنْ قَبْلِ أَنْ يُقْضَى إِلَيْكَ

وَحْيُهُ وَقُلْ رَبِّ زِدْنِي عِلْمًا) (114).

صدق الله العظيم

Dedication

*This work is dedicated to our fathers and mothers
and all family members,*

*To Sudan University, Collage of Petroleum
Engineering And Technology*

*To Teachers and our Colleagues,
And To friends*

Acknowledgement

*We would like to express our greatest thanks to our supervisor **Dr. Alradi Abass**, who has dedicated his knowledge and time, he motivated, guide and support us through all steps of this project, he has been very patient, friendly and very kind with full professional advice.*

*We would also like to express our grateful and worm thanks for Central Petroleum Laboratory staff (CPL) especially for **Mr. Mohamed Ahmed A/Elwahab** (Pet. Eng. Section head) and **Mr. Hytham Gad Almuola** (SCAL & Core Analysis Supervisor) they have dedicated their time, knowledge, contribution and facility.*

*Moreover, especial thanks for GNPOC development department more specific for **Mr. Musaab Almahy** (formation Evaluation T/L) and **Mr. Elbadi Babiker Elbadi** (Senior Reservoir Engineer) they supplied us with three core plugs and data.*

Table of contents

Title	Page No.
CHAPTER 1	
Introduction	1
Mechanisms	2
Objective	3
Problem statement	3
CHAPTER 2	
Theoretical background	4
Literature review	6
CHAPTER 3	
Introduction	8
Methodology	8
Stream Diagram	9
Preparation of core samples	10
Porosity measurement prior saturation	11
Pore Volume Measurement	11
Bulk volume measurement	12
Permeability Measurement	13
Procedure	14
Core imbibition process	17
Brine Preparation	17
Solution preparation	18
Core samples plugs saturant	18
Calculation of brine saturant	19
3.6 Preparation of core plugs for oil saturation	20
Absolute permeability measurement:	20
3.6.2 Saturation core plugs with oil	21
3.7 Core plugs water flooding:	21
Experimental setup	22

3.9 Procedures	22
----------------	----

CHAPTER 4

Result and Discussion	24
-----------------------	----

Introduction	24
--------------	----

Chapter 5

Conclusion	41
------------	----

Recommendations	42
-----------------	----

References	43
------------	----

List of tables

Name of Table	Page No.
TABLE- 4.1 Depth of core plugs	24
TABLE- 4.2 Average diminutions of core plugs (S1)	25
TABLE-4.3 Average diminutions of core plugs (S2)	25
TABLE- 4.4 Average diminutions of core plugs (S2)	26
TABLE- 4.5 Average measurement of Pore Volume for each core plugs	26
TABLE-4.6 Permeability calculation using Darcy law	28
TABLE-4.7 Conversion of apparent permeability (Ka to KL)	28
TABLE-4.8 Calculation of NaCl	29
TABLE-4.9 Calculation of brine saturant	29
TABLE-4.10 Absolute permeability measurement (SN1)	30
TABLE-4.11 Absolute permeability measurement (SN2)	31
TABLE-4.12 Absolute permeability measurement (SN3)	32
TABLE-4.13 Calculation of Initial and Residual Oil Saturation	32
TABLE-4.14 Water flooding base case results (Core No-2)	33
TABLE-4.15 Water flooding ResultsWith Vibration, Core No-2	34
TABLE-4.16 Water flooding base case results Core No-3	37
TABLE-4.17 Water flooding Result With Vibration, Core No-3	38
TABLE-4.18 Relation between Sor before & after Seismic Simulation	40

List of figures

Name of figure	Page No.
Fig. 3-1 Soxhlet Extractor	10
Fig. 3 -2 schematic diagram of helium porosimeter apparatus	12
Fig.3-3 Digital gas permeameter device	14
Fig.3-4-Nitrogen Viscosity as a Function of Temperature	15
Fig.3.5 Automatic Saturator Machine	18
Fig.3-6 Weighting Core Sample in Saturation	19
Fig.3-7Weighting Core Sample in air	19
Fig.3-8 Vibration Generator and Vibration Measurement Devices	23
Fig. 3.9 Vibration Generator attached to Core Holder	23
Fig4 -1 Gas viscosity as a function of temperature.	27
Fig. 4-2Absolute permeability measurement (SN1)	30
Fig. 4-3Absolute permeability measurement (SN2)	31
Fig. 4-4Absolute permeability measurement (SN3)	32
Fig. 4-5 Plot of oil recovery vs. pore volume injected (SN2)	35
Fig. 4-6 Plot of oil recovery (cc) vs. time (min)	36
Fig. 4-7 Plot of Oil Recovery (cc) vs. Pore Volume Injected (SN3)	39
Fig. 4-8 Plot of Oil Recovery (cc) vs. Time (min)	39

Nomenclature

A	Cross sectional area of sample in
B	Constant depending upon the average free movement
C _i	Conductivity of the ith salt
CPL	Central petroleum laboratory
C _s	Conductivity of the solution
D	Pore plug diameter
EOR	Enhanced oil Recovery
GNPOC	Greater Nile Petroleum Operating Company
g _s	Solute's weight (g)
HE-81	Hegleg East -81
K _a	Apparent permeability
K _L	True permeability
K _g	Sample Permeability
L	Core plug length
M	Solution molarity
MMs	Solute molecular weight (g/mol)
N _i	Concentration of ith salt
N _t	Total dissolves solid
P	Pressure
P _A	Atmospheric pressure in atoms
P _V	Pore volume
Δp	Pressure drop

Q	Flow rate
R	Channel radius
S _g	Gas Saturation
S _l	Liquid Saturation
S _o	Oil Saturation
S _{oi}	Initial oil saturation
S _w	Water saturation
S _{wi}	Initial water saturation
ρ _s	Density of saturating liquid
ρ _o	Oil density
V ₁	Volume of the matrix cup without core
V ₂	Volume of the matrix cup with core
V _b	Bulk volume of core
V _g	Volume of grain and non-connected pores
V _m	Matrix volume
∅ _e	Effective (interconnected) porosity of the core
∅ _{sat}	Saturated porosity
μ	Viscosity
W ₁	Water weight
W ₂	Oil weight
W _L	Liquid weight
W _{sat}	Weight of sample in air
W _{sub}	Weight of sample submersed in saturating liquid
WOV	Without vibration

ABSTRACT

Previous theoretical and experimental works described the acoustic stimulation as a potential method for enhancement of oil recovery. Several mechanisms have been suggested to govern the process of additional oil recovery under acoustic energy; nevertheless more research is needed to understand the exact physics behind the process. The main focus of this work is to investigate the effects of ultrasonic waves on oil displacement in porous media at core scale.

To achieve this, an experimental practice investigating (a) oil recovery due to spontaneous displacement of oil by water in 2-D sand pack models, and (b) penetration of ultrasonic waves in different sequences was designed. In each series of experiments the parameters were fixed to monitor only the influence of the ultrasonic wave properties (frequency and intensity). The results helped clarify the effects of ultrasonic energy on oil recovery and - displacement mechanics for different permeability. We were also able to identify some of the governing oil recovery mechanisms caused by ultrasonic energy for different conditions and limiting factors to apply this technology. This work is hoped to be another footstep for research in this area.

المستخلص

أثبتت التجارب والدراسات السابقة ان طريقة الاهتزاز لها الاثر الفعلي في زيادة استخلاص النفط عدة طرق اهتزازية استخدمت لاستخلاص النفط ولكن للحصول على المفهوم الفيزيائي الذي يوضح الآلية الفعلية التي يتم من خلالها الحصول على زيادة في إنتاج النفط المتبقي نوصي بزيادة الدراسة والبحث في هذا الموضوع.

تم أداء عدة تجارب معملية لدراسة اثر الموجات الاهتزازية في زيادة استخلاص النفط علي عدة عينات من الصخر ذات مواصفات معملية مختلفة (مختلفة النفاذية) لتحقيق مفهوم التجربه المعملية عن طريق الازاحة بالماء في عينه من الصخر تم تسليط موجات ذات تردد مختلف عند ثبوت الخصائص الاخرى وذلك ساعد علي استخراج النفط المتبقي من عينات ذات نفاذية مختلفة. من المؤمل ان تكون هذه الطريقة تحت الدراسة والبحوث.

CHAPTER 1

Introduction

CHAPTER 1

1.1 Introduction:

Oil is still playing the most prominent role in providing energy for the thirsty industrial world and the prospect of near future does not show any major resource to take its place. High demand for oil and rising trend of oil prices have urged oil companies to search for newer and more efficient ways of oil production. Natural driving forces responsible for primary recovery such as reservoir pressure and gravity forces usually produce a small fraction of original oil in place, especially in reservoirs with unfavorable conditions such as low oil gravity and oil-wet rocks. After secondary recovery, e.g. water flooding, there could still be a large amount of oil remaining in such reservoirs. Various methods of enhanced oil recovery have been introduced to maximize oil production. They may not be suitable for every type of reservoirs either due to economical or technical limitations. Therefore, many different unconventional techniques have been proposed and even tested in the field conditions. Use of acoustic energy to stimulate oil reservoirs is a potential method which, at the first glance, might seem a mechanical stimulation. This, however, needs profound research to reveal the physics of the process and mechanisms involved in oil recovery under acoustic energy. Looking at previous works in this area, we designed 2 and performed a number of experimental works to obtain a better insight into the subject particularly on the effects of ultrasonic waves on oil displacement and recovery. There are some advantages of using elastic sound waves to improve oil recovery. For example, it is environmentally friendly and, from the recovery point of view, it is an efficient way to distribute the energy in all directions in a medium due to its spherical transmission. Its major limitation, on the other hand, appears to be the rapid attenuation of high frequency waves through porous media because of shorter wavelengths. The impact of high frequency waves is expected to be more critical at pore scale. The mechanisms of stimulation in porous media by elastic waves are not well understood yet. This requires more physical experimentation especially at core/pore scale. Introduction of ultrasonic energy (high frequency sound waves) as a stimulation method dates back to early 60's. Studies done over this period of time are still limited to disclose the physics that governs the process to improve oil recovery, especially from liquid-liquid and solid-liquid interaction under ultrasonic point of view.

1.2 Mechanisms of ultrasonic energy

Understanding the governing mechanisms is important for field applications. In general EOR process the proposed mechanisms related to capillary forces is peristaltic movement due to the pore walls deformation imposed by mechanical vibration, capillary forces reduction due to weakening of surface films at pore boundaries, coalescence of oil drops due to the Bjerknes forces, oscillatory movement of oil drops trapped by capillary forces, forces from bubble cavitations and capillary effect which is the increase of depth of fluid penetration into pores in an ultrasonic field (Malykh et al. 2003). Mechanical vibrations generated by ultrasonic waves influence interfacial forces and increase the relative permeability of the phases. At high intensities ultrasonic waves can also decrease the wetting films adherence to the matrix. Moreover, the heat generated due to vibration generated by ultrasonic waves reduces viscosity, density and surface tension. In the presence of surfactants, ultrasonic energy helps emulsification of oil. The vibration may lead to deformation of pore walls which will increase permeability and the porosity of rock. This vibration can also help removing the fines, clays and asphaltenes from pores. These mechanisms depend on both medium (rock and fluid) and wave properties. Parameters such as rock elasticity, porosity, fluid viscosity, surface tension, wave frequency and intensity determine the viability of the mechanisms. For example, wave penetration and its ability to make pores walls deformation are highly dependent on its frequency and power (intensity). Experimental works at core and pore scale is still needed to investigate the influence of ultrasonic waves on these parameters in the context of incremental oil recovery. It is also critical to identify under what circumstances (or for which type of reservoirs) this technique becomes more suitable, but due to no advance laboratory & models available the effect of ultrasonic waves on previous parameters not measured in our project, only we measure the effect of the ultra-sonic waves on oil recovery.

1.3 Objectives

- The objective of this project is to demonstrate the impact of downhole vibration stimulation on production rates in a mature water flooded reservoir, by physical simulation lab experiments of actual reservoir behavior of Heglig Area as Case study.
- To study the effect of permeability variation on ultra-sonic waves technique.
- To study the influence of vibrations time on oil recovery factor.

1.4 Problem statement

In some cases seismic stimulation increased production rates by 20% or more, but in other cases production was unchanged or actually declined. This is primarily due to the fact that historic laboratory and field experimental data are not comprehensive enough to allow reliable prediction of the physical conditions under which stress wave stimulation is most effective despite of application of EOR methods (water flooding) in Heglig field still considerable amount of recoverable oil can be obtained by the vibration stimulation.

CHAPTER 2

Theoretical Background And Literature Review

CHAPTER 2

2.1 Theoretical background

The idea of using elastic wave method to improve oil recovery returns back to the 1950s. The very first research study in this area was reported in 1965. Duhon and Campbell (1965) conducted water flooding tests on cores under ultrasonic energy with frequencies of 1, 3.1, and 5.5 MHz. The injection point was at the center of a sandstone core in which the ultrasonic probe was also introduced. A receiving probe was placed at the end of the core. Their study showed that the ultrasonic energy improved the oil recovery and displacement efficiency in the cores. They also observed that by increasing frequency, the cavitation and recovery decreases. In the next three decades, the attention was devoted to elastic wave stimulation on oil recovery by seismic waves which have smaller frequencies than ultrasound waves. Beresnev and Johnson (1994) compiled and well documented all these efforts and provided a comprehensive review of methods using elastic wave stimulation of oil production, including both ultrasonic and seismic methods. What they concluded after this review was that the elastic wave and seismic excitations to porous media affect permeability and production rate in most cases. They also listed laboratory cases that focused on the influence of seismic and ultrasound waves on the different characteristics of fluids, porous structure, and oil recovery. Among them there were a few ultrasonic cases. Nosov (1965) observed a decrease in the viscosity of polystyrene solution under sound waves. Pogosyanetal. (1989) showed that gravitational separation of water and kerosene accelerates due to acoustic field. In addition to laboratory research, Beresnev and Johnson (1994) then pointed out four case studies of downhole reservoir ultrasonic stimulation. (1992) applied ultrasonic radiation in two field tests in California which stimulated oil production remarkably. Ganiev. (1989) proposed that ultrasound would deform the pore walls and alter the radius of the pore. This vibration causes fluctuations in capillary pressure and expansion of surface films. Traveling waves along pore walls may cause a “peristaltic transport” of fluid displacement. This can be a possible explanation for permeability changes observed by Cherskiy et al. (1977). More recently, Aarts and Ooms (1998) stated that mechanism of peristaltic move works only at ultrasonic frequencies, and also the amount of the ultrasonic field should be more than a specific

amount. With these conditions, the effect will happen only near well bore due to the high attenuation of ultrasound. Later, Aarts et al. (1999) showed that ultrasonic radiation deforms the pore walls and enhances the fluid velocity in porous media. They used a rubber stopper as the porous medium and water as the fluid and a 20 kHz ultrasonic source. They analyzed the “peristaltic transportation” mathematically. Their both numerical and experimental results showed that, by increasing ultrasonic power, the velocity of fluid inside the porous media increases. They suggested that ultrasonic energy may assist well acidizing. The positive effect of vibration on oil recovery was demonstrated and it was attributed to the restoration of permeability as a result of drop 10 clusterization. A mathematical model was also proposed to illustrate the dominant vibration frequency. Such model is based on the nonlinear effect associated with viscoelastic resonance. Elastic wave fields may reduce the capillary forces by vibrating, and consequently, breaking surface films adsorbed to pore walls. Ultrasonic vibrations may mobilize oil droplets into pores, or may result in coalescence due to the Bjerknes forces. Dunin and Nikolaevskii (2005) and Nikolaevskii and Stepanova (2005) proposed a theory about the ultrasonic waves generation as result of nonlinear effects associated with seismic and low frequency acoustic waves in porous media saturated with fluid. Li et al. (2005) studied the mobilization of oil ganglia in a 2D etched glass micro-model under low frequency vibrations. They observed an increase in the recovery with higher amplitude and lower frequency. Residual oil is entrapped as ganglia in narrow pores because of resisting capillary forces. Beresnev et al. (2005) showed that vibrations help overcome this resistance. Adding vibratory forces to the external gradient makes instant unplugging of entrapped ganglia occur. Their experiments on glass micro-model along with computational simulation showed that the mobilization of residual saturant of ganglia is proportional to the amplitude and inversely proportional to the frequency. In their penetration zone, acoustic waves can have big effects on fluid-matrix interaction and therefore hydrocarbon displacement and recovery. This effect as well as the propagation distance is highly dependent on wave frequency and intensity. High frequency ultrasonic waves put a limitation in their effective penetration radius; hence many researches focused on low frequency stimulation (seismic stimulation) (Simonov et al. 2000; Kuznetsov et al. 2002, Kostrov and Wooden 2005) and also pressure pulsing technology (Dusseault et al. 2000, Spanos et al. 2003).

2.2 Literature review:

Robert Westermarck (2003) has published report on applying pilot project of downhole vibration stimulation after applying the technology on osage county Oklahoma field. The field was already being subjected to water flooding. Vibration tool was lowered in a new drilled well, and down hole vibration strength was also monitored in the adjacent wells, unfortunate the project was not successful due to mechanical pre-mature failure of the vibration tool (after 4 from start the vibration). They also conducted laboratory experimental portion of their project utilized a core test cell with a magnetostrictive actuator applying mechanical stress excitation to sandstone core samples during single-phase and two-phase fluid flow, also apply the mechanical vibration to core plugs after establishing the residual oil saturation through water flooding injection.. Results indicate that mechanical stress excitation at 100 Hz and lower can strongly influence two-phase fluid flow behavior in Berea sandstone under both steady state and simulated flood conditions.

Mihailo Jankov (2010) investigated the effect of tunable seismic vibration on two phase flow in the porous medium. His quasi two-dimensional synthetic porous medium consists of a monolayer of 1 mm diameter glass beads between two sheets of transparent contact paper florescence photo could be taking during the experiment process. The porous medium was set horizontally so the effect of gravity was excluded and only effect of capillary and viscosity forces was the controlling factors. In the setup he used two immiscible phase fluids wetting phase displacing non wetting phase fluids. He stated his observation that when the vibrational stimulation is applied the invading cluster geometry changes regardless to the direction that depending on the oscillatory frequency and the acceleration amplitude. Derived a scaling relation relating pressure, saturation, system size and capillary number Ca . And by applying this pressure-saturation scaling relation, curves for a range of capillary numbers have been collapsed onto a system size- and Ca - independent master capillary curve.

Beresnev and Johnson (1994) provide a review of both the field evidence for and possible physical mechanisms behind seismic stimulation. On the theoretical front, Hilpert et al. (2000), Lassonov and Beresnev (2003), Beresnev et al. (2005), Bere (2006), and Hilpert (2007) give

analytical models for how a single bubble stuck in a capillary tube might be mobilized if the capillary walls are shaken by a passing sound wave.(**Seismic stimulation for Enhanced Oil Recovery**)

Peter M. Roberts et al. (2002) Said that it has been observed repeatedly that low-frequency (10-500 Hz) seismic stress waves can enhance oil production from depleted reservoirs .In some cases seismic stimulation increased production rates by 20% or more, but in other cases production was unchanged or actually declined. This is due primarily to the fact that historic laboratory and field experimental data are not comprehensive enough to allow reliable prediction of the physical conditions under which stress-wave stimulation is most effective.

CHAPTER 3

Methodology

CHAPTER 3

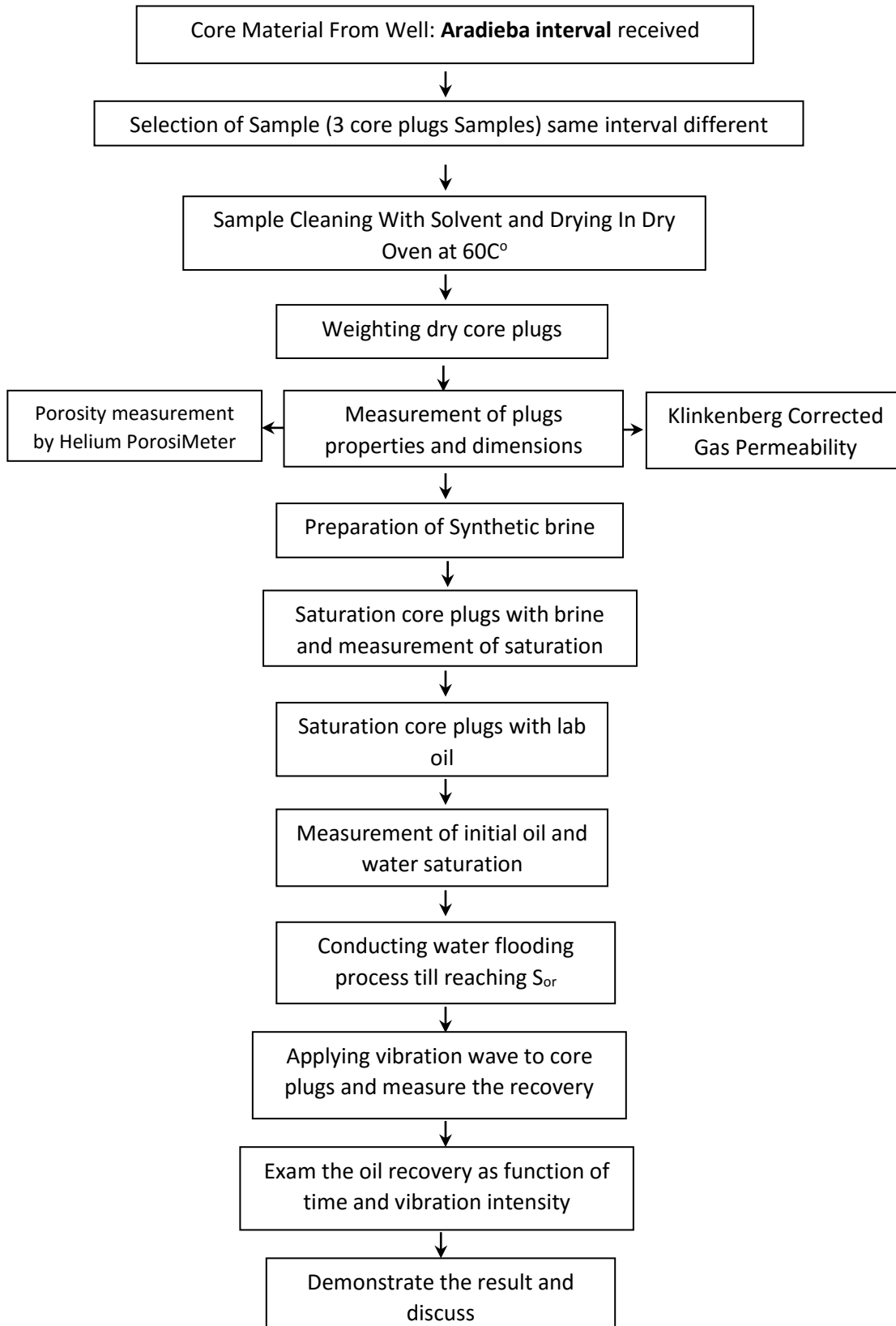
3.1 Introduction:

This chapter illustrates all Processes that should be carried out on core plugs which include core plugs cutting, cleaning, measurement of properties and saturation processes that in order to prepare the plugs so as to perform the study of seismic stimulation.

3.2 Methodology

To investigate the effects of seismic waves on oil recovery and displacement of oil from core plugs while water flooding, two series of lab tests have been designed under same conditions, but the cores have different properties (i.e. porosity and permeability...etc). First, a core plugs must be saturated by synthetic brine or with formation water and then laboratory oil (ISO-bar) to be injected into the core plugs so as to simulate reservoir at initial conditions (drainage process). Then imbibition process is should be performed (core experiments) to recognize the effect of water flooding on oil recovery. when 100% water cut achieved, vibration should be started immediately and gradually. The vibration source generates an ultra-sonic waves measured by **vibrotip** (vibration intensity meter) for three different frequencies. This way the effect of ultrasonic energy on enhance oil recovery can be identified. The main goal of this practice is to study the effect of seismic stimulation in mobilizing bypassed and trapped oil from rock porous that in turns increases oil recovery, and compare the obtained recovers to the oil recovered by the water flooding without vibration. The experimental practices were designed in such a way that the effect of ultrasonic waves in various frequencies on oil recovery and water flooding displacement can be identified.

3.3 Stream Diagram:



3.4 Preparation of core samples

3.4.1 Core plugs cleaning:

The weight of each core plug was initially recorded. Core plugs were immersed in methanol inside piker for 18 days, so as to extract the oil from the cores. After then plugs were re-loaded into ,Soxhlet extraction apparatus, for two weeks, this is the most common method for cleaning sample, toluene is brought to a slow boil in a Pyrex flask; its vapors move upwards and the core becomes engulfed in the toluene vapors (at approximately 1100C°). Eventual water within the core sample in the thimble will be vaporized. The toluene and water vapors enter the inner chamber of the condenser; the cold water circulating about the inner chamber condenses both vapors to immiscible liquids. Re-condensed toluene together with liquid water falls from the base of the condenser onto the core sample in the thimble; the toluene soaks the core sample and dissolves any oil with which it come into contact. Also salts between the grains was removed.

The Dean-Stark distillation provides a direct determination of water content. The oil and water area extracted by dripping a solvent, which is toluene. This is to calculate the water weight and oil weight removed from the core plugs, the water and solvent are vaporized and re-condensed in a cooled tube mounted on the top of the apparatus and the water is collected in calibrated chamber therefore water volume is recorded and its weight can be determined, oil content can be calculated by the difference between the weight of water recovered and the total weight loss after extraction and drying. Pore volume and saturation of liquid was determined. (Laboratory wok book, O. Torsæter M. Abtahi).

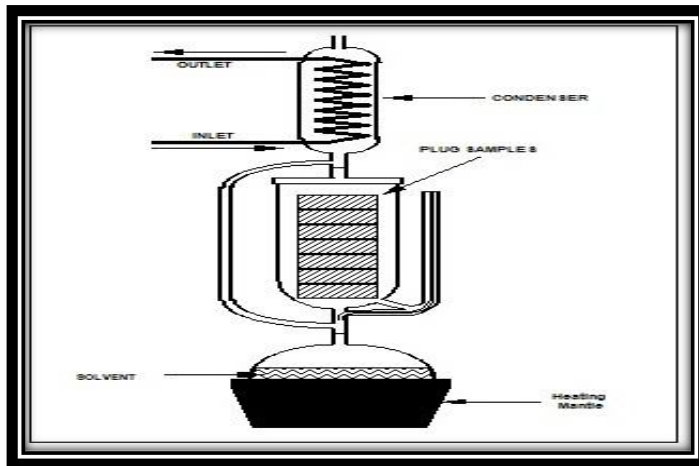


Fig. 3-1 Soxhlet Extractor *(laboratory work book, O. Torsæter M. Abtahi)

$$W_L = W_1 + W_2$$

3-1

W_L = liquid weight.

W_1 = water weight

W_2 = oil weight.

$$W_1 = \frac{\text{density}}{\text{volume}}$$

3-2

W_L = sample weight wet- sample weight dry

$$W_2 = W_L - W_1$$

3-3

$$V_{\text{oil}} = \frac{W_2}{\rho_o}$$

3-4

ρ_o = oil density (given by company)

$$S_L = \frac{V_L}{P.V}$$

3-5

S_L = liquid saturation

P.V = pore volume cm^3

3.4.2 Porosity measurement prior saturation:-

After the cleanness of the core plugs, determination of rock properties was carried out in the core properties laboratory. The device which was used for this process is called Digital Helium PorosiMeter. And the steps as follows;-

3.4.3 Bulk volume measurement:-

The dimensions of each plug were measured through the use of digital Venier, six readings recorded for both length and diameter from six different positions of the plug and average reading is calculated for the six reading (Tables 4-2, 4-3, and 4-4).

$$\text{Bulk volume} = \left(\frac{\pi D^2}{4} \right) * L$$

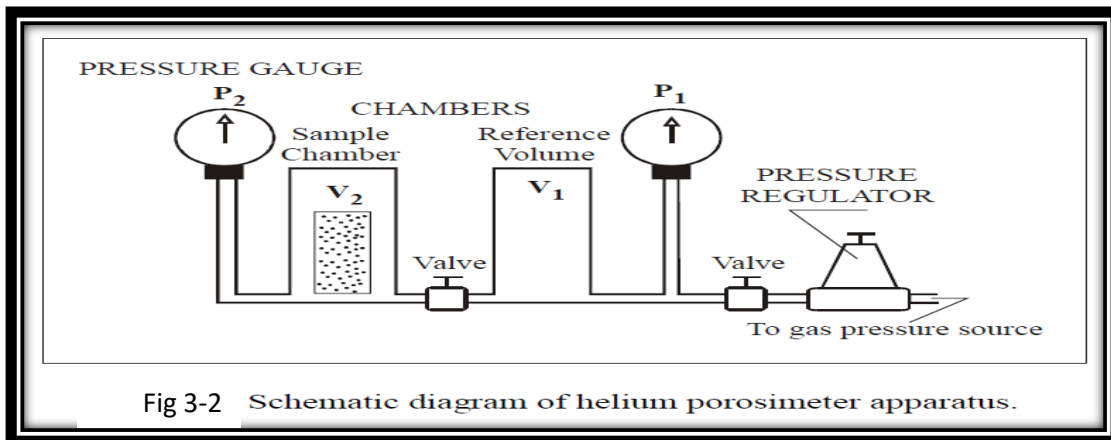
3-6

L = core plug length (cm)

D = core plug diameter (cm)

3.4.4 Pore Volume Measurement:

Measurement of porosity and grain volume that was measured through the use of helium technique method which employs Boyle's law, (Digital Helium Porosimeter Fig. 3-2) The device has a reference volume V_1 , at pressure p_1 , and a matrix cup with unknown volume V_2 , and initial pressure p_2 . The reference cell and the matrix cup are connected by tubing; the system can be brought to equilibrium when the core holder valve is opened, allowing determination of the unknown volume V_2 by measuring the resultant equilibrium pressure p . (Pressure p_1 and p_2 are controlled by the operator; usually $p_1 = 100$ and $p_2 = 0$ psig). When the core holder valve is opened, the volume of the system will be the equilibrium volume V , which is the sum of the volumes V_1 and V_2 . Boyle's law is applicable if the expansion takes place isothermally. Thus the pressure-volume products are equal before and after opening the core holder valve. (Table 4-5)



(laboratory work book, O. Torsæter M. Abtahi)

$$P_1 V_1 + P_2 V_2 = P (V_1 + V_2)$$

3-7

Solving the problem to unknown V_2 :-

$$V_2 = (P - P_1) * \frac{V_1}{P_2 - P}$$

3-8

Since P_2 is zero and $P_1 > P$ the equation is simplified to be:-

$$V_2 = (P_1 - P) * \frac{V_1}{P}$$

3-9

V_1 = the volume of the reference cell (cm^3).

V_2 = the unknown volume in the matrix cup (cm^3).

P_1 = the reference cell pressure (psig).

P_2 = the sample chamber pressure which is Zero (psig).

P = pressure read directly from the gauge (psig).

Calculations

V_1 = the volume of the matrix cup without core, cm^3 .

V_2 = the volume of the matrix cup with core, cm^3 .

$V_g = V_1 - V_2$, the volume of grain and non-connected pores, cm^3

V_b = the bulk volume of core, cm^3 .

$\phi_e = (V_b - V_g) / V_b$ effective (interconnected) porosity of the core, *fraction*

$$\text{Pore volume} = \text{bulk volume} - \text{grain volume}$$

$$\text{Porosity} = \frac{\text{pore volume}}{\text{bulk volume}} * 100 \quad \boxed{3-10}$$

$$\text{Grain volume} = \frac{\text{weight}}{\text{grain density}} \quad \boxed{3-11}$$

(Laboratory work book, O. Torsæter M. Abtahi-2000)

3.4.5 Permeability Measurement:

Permeability is measured by passing a fluid of known viscosity through a core sample of measured dimensions and then measuring flow rate and pressure drop (table 4-14) illustrated the pressure drop across sample and flow rate measurements. Various techniques are used for permeability measurements of cores, depending on sample dimensions and shape, degree of consolidation, type of fluid used, ranges of confining and fluid pressure applied, and range of permeability of the core.

Permeability tests are performed on samples which have been cleaned and dried and a gas (usually air) is used for flowing fluid in the test. This is because:

1. Steady state is obtained rapidly.
2. 100% fluid saturation is easily obtained.

Constant Head Permeameter:

This equipment is designed for plug permeability measurements. Hassler core holder may be used with this instrument. The Hassler system is an improvement of the rubber plug system whose tightness is limited at certain pressures. The core is placed in a flexible rubber tube. The Hassler cell has these advantages:-(laboratory work book, O. Torsæter M. Abtahi-2000).

- 1- Excellent tightness.
- 2- Can be used for samples of different sizes.
- 3- Much higher pressure or ΔP can be used.

Procedure:

The measured nitrogen permeability is influenced by the mean pressure P_m of the core. The mean pressure is regulated by the upstream and downstream valves on the sides of Hassler cell. The rate is measured at atmospheric conditions with a mass flow meter in percent of maximum rate which is 200 l/hour. Nitrogen viscosity as a function of temperature is shown in the **Fig.3-4**.



Fig.3-3 Digital gas permeameter device

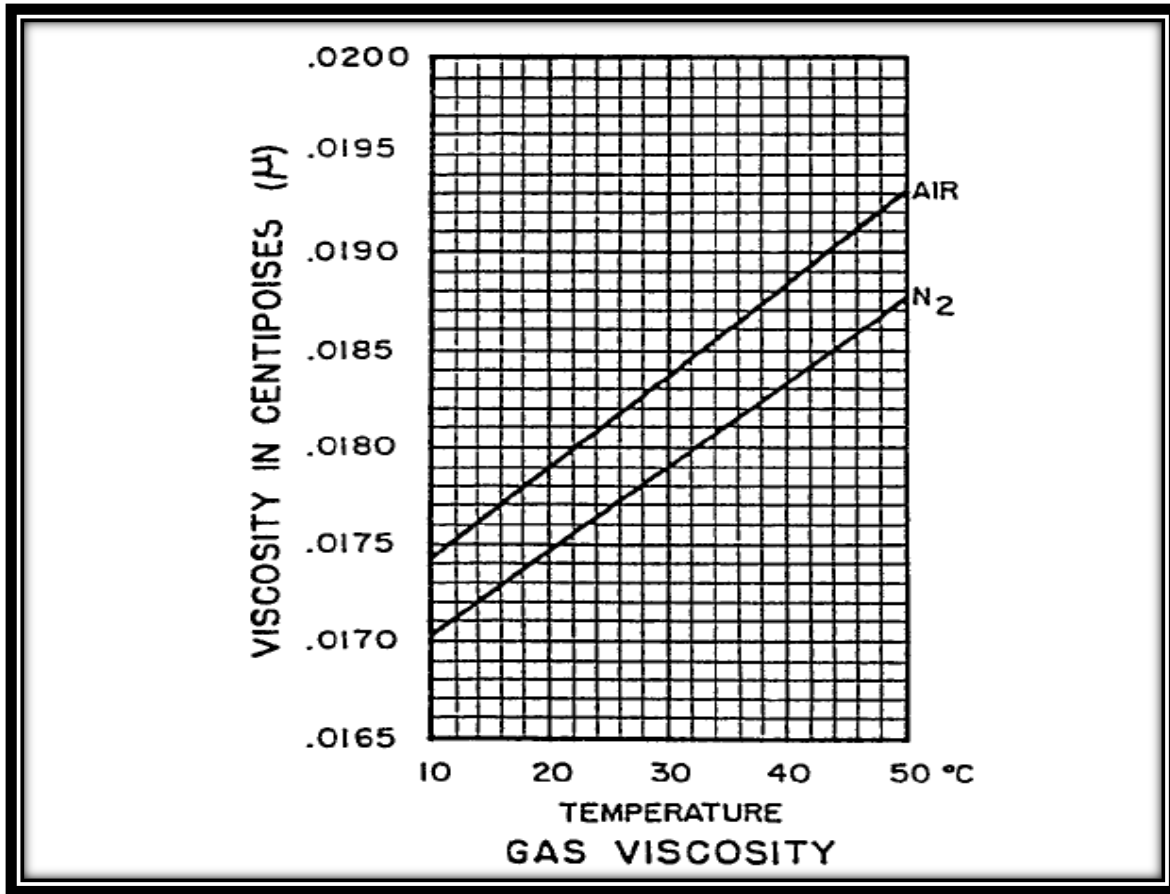


Fig.3-4-Nitrogen Viscosity as a Function of Temperature

(laboratory work book, O. Torsæter M. Abtahi-2000)

Four measurements of nitrogen permeability were taken at different pressures. It was important to keep the ΔP constant, because the air flow at the core sample must be laminar. It is best to have relative little pressure difference, ΔP so as to avoid turbulent flow. Darcy's equation may be used for determining permeability of liquids. The volumetric flow rate q is constant for liquids, because the density does not change during flow through the core.

$$Kg = \frac{Q \times \mu \times P_A \times L \times 2000}{A \times [(P_1 + P_A)^2 - (P_2 + P_A)^2]} mD$$

3-12

Where:

L =Length of sample in cm

D =Diameter of sample in cm

A =Cross sectional area of sample in $\text{cm}^2 = (D/2)^2 \times \pi$

μ =Viscosity of gas in centipoises (at known temperature)

P_A =Atmospheric pressure, atm

P_1 =Corrected upstream pressure, atm

P_2 =Corrected downstream pressure, atm

Q =Flow rate in cc/s

The length and diameter of the sample was measured using calipers and gas permeability was calculated using Darcy law(Table 4-6).

Klinkenberg has related apparent permeability k_a measured for gas for an average pressure P_m to the true permeability k_L by:

$$K_a = K_L * \left(1 + \frac{b}{P_m}\right) \quad 3-13$$

Where b is constant depending upon the average free movement λ of the molecule at P_m

$$b = \frac{4C'\lambda P_m}{r} \quad 3-14$$

Where r is channel radius and $C' \cong l$.

Conversion of K_a to K_L by Formula(table 4-7) shows the results

If $K_g < 100$

$$K_L = 0.68 * K_g^{1.061}$$

If $K_g > 100 < 400$

$$K_L = 0.68 * K_g^{1.056}$$

If $K_g > 400$

$$K_L = K_g \left(\left(\frac{K_g}{1000} * .005 + .95 \right) \right) \quad 3-15$$

(laboratory wok book, O. Torsæter M. Abtahi-2000)

3.4.6 Core imbibition process:-

The imbibition process is performed in the laboratory by first saturating the core with water (wetting phase), then displacing the water to its irreducible (connate) saturation by oil injection. This “drainage” procedure is designed to establish the original fluid saturations that are found when the reservoir is discovered. Then the wetting phase (water) is reintroduced into the core and its saturation continuously increased. This is the imbibitions process and is intended to produce the relative permeability data needed for water drive or water flooding calculations.(Res. Eng.Tarig A.)

3.4.7 Brine Preparation:-

Synthetic brine was prepared at the lab, the formation salinity was given by the company (GNPOC) Petrophysics which is(1792.96mg/l).Accordingly the brine salts concentration was calculated. The concentration is usually referred to as the equivalent NaCl concentration.(Table 4-8)

1- Calculation of NaCl

The conductivity of the solution can be estimated with a sufficient accuracy by

$$C_s = \frac{1}{nt} \sum_{i=1}^N n_i C_i \quad 3-16$$

C_s : conductivity of the solution (ohm/m).

nt :- Total dissolve solid (ppm) TDS.

n_i :- Concentration of i^{th} salt (ppm).

C_i : Conductivity of the i^{th} salt.

Calculation of grams of solute required:-

$$g_s = MM_s * M * V \quad 3-17$$

g_s = solute's weight(g).

MM_s = solute molecular weight (g/mol).

M = solution molarity (mol/l)

3.4.8 Solution preparation:-

- 5 liter of fresh water was distilled by using water neutralizing device (Micromeg device) and then stored in clean bottle.
- NaCl amount required for the solution is weighted by using 0.5 μ m meter.
- 75% (3liters) of the distilled water poured into a glass flask and then placed on the stirring unit.
- 6.16g of NaCl was added to the stirring 3 liters of water.
- The left 2 liters of neutralized water was poured into the glass flask.
- The flask was covered and then left stirring for one hour to ensure the mixture homogeneity.
- After then the solution was filtered through 0.45 μ m pore size filter.
- While the solution being stirred, dissolved gasses was extracted through applying vacuum to the degassing pan by vacuum machine for 24hr.
- The brine now is ready for the saturant.

3.4.9 Core samples plugs saturant

Dry Core plugs weights were measured again prior saturating them by brine, the core plugs were saturated in Automatic saturator machine steps as follows:-



Fig.3.5 Automatic Saturator Machine

- Core samples plugs placed on the core seat and then placed into the saturator cell.
- Core saturator cell was firmly closed.
- Air inside the core saturator cell and inside the porous was removed by vacuum pump until the vacuum pressure reached -14.696psi.
- Now the saturator cell valve open for the brine to flow into the cell, after the cell pressure reached zero psi the pressure maximizing pump started to increase the saturator cell pressure till 1763psig.
- The core saturator left under this pressure for 24hrs after then core plugs was removed out the cell and brine saturant measurement as follows.
- Saturated core plugs weighted in air, through the use of 0.5 μ m meter.
- Saturated core plugs were immersed in saturant and weight was recorded.
- Cores plugs were already weighted dry before saturant.
- The brine density measured and found 1.0023g/cc

3.5.1 Calculation of brine saturant:-

Archimedes method is applied where the brine saturated core plugs were weighted wet in air and weighted immersed in Saturation. (Table 4-9)



Fig.3-6 Weighting Core Sample in Saturant



Fig.3-7 Weighting Core Sample in air

$$Pv = \frac{W_{sat} - W_{dry}}{\rho_{sat}} \quad 3-18$$

$$Vb = \frac{W_{sat} - W_{sub}}{\rho_{sat}} \quad 3-19$$

$$Vm = \frac{W_{dry} - W_{sub}}{\rho_{sat}} \quad 3-20$$

$$\phi_{sat} = \frac{W_{sat} - W_{dry}}{W_{sat} - W_{sub}} \quad 3-21$$

(laboratory wok book, O. Torsæter M. Abtahi-2000)

Where:-

- V_b = bulk volume.
- Pv = pore volume.
- V_m = matrix volume.
- $W_{sat.}$ = weight of sample in air (100% saturated).
- $W_{sub.}$ = weight of sample submersed in saturating liquid .
- ρ_s = density of saturating liquid.
- ϕ_{sat} = saturated porosity.

3.6 Preparation of core plugs for oil saturation:-

After saturation core plugs with brine, and measuring the pore volume saturated by brine, then the core plugs were loaded into the core holder, air inside the core holder was removed, and then a confined pressure of 523psi was applied on the core plugs after then the flow of brine was injected into the plugs at three different flow rates and the differential pressure across the core plug was recorded this is to calculate the absolute permeability of the core plugs by using brine.

3.6.1 Absolute permeability measurement:

In the process injection of brine was done at three different flow rates and the differential pressure of each flow rate was recorded and then plotting the ratio of flow rate to area (q/A) versus the pressure function ($\Delta p/L$) as shown in (Tables 4-10, 4-11 4-12).

3.6.2 Saturation core plugs with oil:

Introducing the synthetic laboratory oil has viscosity of 1.565cp into core plugs. Oil was injected into the core plugs at constant pumping rate and the displaced brine volume was collected in a scale graded tube. Oil volume pumped into the core was ten times the core plug pore space this is to ensure that no more water brine can be displaced, thus the initial oil and water saturation (S_{oi} and S_{wi}) were established. (Table 4-13)

$$S_{wi} = \left(\frac{\text{Pore volume - squeezed - cumulative water produce}}{\text{pore volume - squeezed}} \right) * 100 \quad 3-22$$

- Squeezed is the volume of water brine (cc) that displaced out of core plugs due to the confined pressure exerted on the plugs and it is a function of the amount of the confined pressure. The squeezed volume received in the graded tube is 0.59cc.
- Cumulative water produce is the water volume displaced by oil.

The initial and residual oil saturation can simply be calculated from the equations below:

$$S_{oi} + S_{wi} + S_{gi} = 1 \quad 3-23$$

$$S_{or} = S_{oi} - S_o \quad 3-24$$

S_{gi} = Zero (no gas saturation), so: $S_{oi} = 1 - S_{wi}$

3.7 Core plugs water flooding:

After injection of oil into the core plugs samples that in order to establish initial oil and water saturation, core plugs were flooded by the same water (Brine) that was used for the saturation. The goal of this step is to investigate the oil recovery that can be obtained by water flooding without exposing the plugs to vibration and to establish the residual oil saturation S_{or} , which can be calculated from the below equation.

Residual Oil Volume (G_r) = initial oil in place – cumulative oil produced

$$G_r = (S_{oi} * PV) - G_{op} \quad 3-25$$

$$\text{Recovery factor} = \left(\frac{G_r}{G} \right) \quad 3-26$$

S_{or} = Recovery factor * initial oil saturation

$$S_{or} = \frac{G_r}{P.V} \quad 3-27$$

Where:-

G_r = residual oil volume cc.

G = initial oil in place cc.

G_p = cumulative oil produced cc.

R.F= recovery factor.

S_{or} = residual oil saturation.

P_v = pore volume cc.

3.8 Experimental setup:

In this step the core plugs samples which are placed inside core holders will be exposed to ultrasonic waves that generated through a use of vibration source. The vibration generation source is attached to core holder and the intensity of the vibration is measured by vibration meter (**vibrotip**) attached to core holder too, the frequency of waves (vibration) is measured in unit of hertz (inch/sec).

The process is to continuo water flooding into core plugs after achieving the residual oil saturation (100% water production), and applying the ultrasonic waves to the core plugs in the same time, alteration of waves intensity will be applied in order to investigate the effect of waves intensity and to determine the appropriate and suitable frequency for the rock. Fig. (3-8 and 3-9) Show vibration measurement device and vibration generator attached to core holder for experiments. Two experiments with low power output to high performed to observe the effect of frequency

3.9 Procedures:

For each case, two experiments were run with and without ultrasonic energy for comparison. imbibition process was started after core prepared and S_{wi} & S_{oi} were measured and vibration source connected to the core holder. Water flooding was started using pharmacy pump for injection a brine (NaCl) at constant flow rate for each cores, and pressure drop (dp) is recoded the and S_o against the time until S_{or} (residual oil saturation) was established .



Fig.3-8 Vibration Generator and Vibration Measurement Devices.



Fig. 3.9 Vibration Generator attached to Core Holder.

CHAPTER 4

Results and Discussion

CHAPTER 4

Results and Discussion:

Introduction: -

This chapter demonstrates the results of routine special core analysis and oil recovery gained as responses for Applying vibration stimulation which was conducted at central petroleum laboratory (CPL) on core plugs taken from HEGLIG field Well **HE-81**, Aradieba interval (Sand Stone Formation) (1426.86 ft to 1434.69 ft). Three Core plugs that used for ISS test were drilled and taken exactly from depth of (table-4.1) to study the effect of In-situ seismic stimulation on oil recovery. Data from routine property measurements are described and presented. Special core analyses consisted of tests to measure oil recovery without and with sonic stimulation (**with respect to various intensities of vibration frequencies**). Limited (due less core plugs tested and limited tests of various rock properties measurement that have been conducted during the process) results from waterfloods without and with sonic stimulation provide evidence that oil recovery was improved as a result of vibration stimulation compared to waterflooding results without vibration stimulation.

TABLE- 4.1 Depth of core plugs

Sample No.	Depth(m)
1	1430.04
2	1432.34
3	1434.00

Table 4-1 shows the exact depths from which the core plugs were drilled.

-High variation of cores permeability's have been noticed and come out as a result, core number three has higher permeability so it achieved higher produced liquids during the experiment.

- Considerable increment of oil recovery has been observed when cores plugs were subjected to vibration, Figures 4-1&4-2.illustrated oil recovery with and without vibration for SN2 and SN3.

Where TABLES-4.14, 4.15, 4.16, 4.17 represent the data obtained from lab experiments on two cores (2,3) with and without vibration, which have been used for plotting these figures.

-The vibration duration has significant effect on oil recovery (more vibration time, more oil recovery);this relationship is illustrated in Figure 4-2&4-2

TABLE- 4.2 Average diminutions of core plugs (S1)

Sample No	Reading	Reading	Reading	Reading	Reading	Reading	Average	Bulk
S1	1	2	3	4	5	6		volume cc
Length(cm)	5.248	5.250	5.257	5.255	5.253	5.263	5.254	61.626
Diameter(cm)	3.877	3.856	3.864	3.870	3.858	3.867	3.865	

TABLE-4.3Average diminutions of core plugs (S2)

Sample No	Reading	Reading	Reading	Reading	Reading	Reading	Average	Bulk
S2	1	2	3	4	5	6		volume cc
Length cm	4.948	4.943	4.952	4.940	4.935	4.944	4.944	56.956
Diameter cm	3.823	3.831	3.823	3.837	3.841	3.831	3.831	

TABLE-4.4 Average diminutions of core plugs (S2):

Sample No	Reading	Reading	Reading	Reading	Reading	Reading	Average	Bulk
3S	1	2	3	4	5	6		Volume _{cc}
Length _{cm}	5.606	5.641	5.669	5.648	5.611	5.601	5.629	65.416
Diameter _{cm}	3.833	3.853	3.854	3.852	3.844	3.849	3.848	

Tables 4-2, 4-3 and 4-4 show the measurement of core plugs length and diameters six measurements for each dimension were taken and the average for the each dimension was calculated, this is for more accuracy.

Table 4.5 average measurement of Pore Volume for each core plugs

SN	Weight (g)	Bulk Volume (cc)	Grain Volume (cc)	Pore Volume (cc)	Porosity %	Grain density (g/cc)
1	123.350	61.63	46.73	14.9	24.17	2.63
2	113.610	56.96	43.12	13.84	24.29	2.63
3	121.990	65.42	46.04	19.38	29.62	2.64

Table 4.5 show the result of pore volumes calculated by the average measurement of core plugs dimensions (length and diameter).

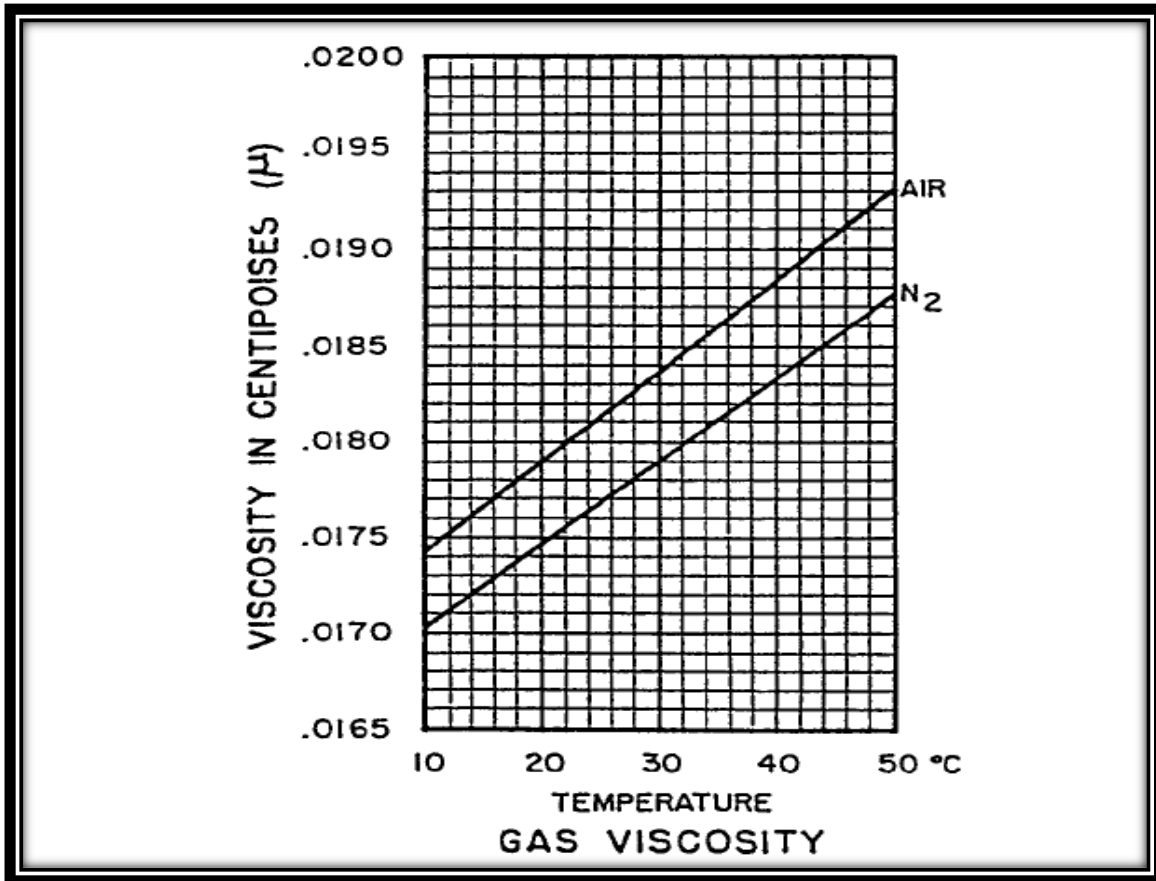


Fig4 -1 Gas viscosity as a function of temperature .

The Fig. 4-1(laboratory wok book, O. Torsæter M. Abtahi-2000) shows the relationship between temperature and the viscosity of nitrogen and air, the viscosity of N₂ and Air increases with temperature at given pressure.

TABLE-4.6 Permeability calculation using Darcy law

S.N	Length (cm)	Diameter (cm)	Temp. (°C)	Atmos. Pressure (mmhg)	Upstream Pressure (psi)	Bulk Volume (cc)	Mass Flowrate (g/sec)	Volum. Flowrate (cc/sec)	Ka (mD)
1-S	5.254	3.865	20.2	760	8.46	61.657	0.0002009	0.1726673	1.830
1-S	5.254	3.865	19.9	760	8.50	61.657	0.0002032	0.1744288	1.837
1-S	5.254	3.865	19.9	760	8.52	61.657	0.0002036	0.1747518	1.835
2-S	4.944	3.831	20.2	760	2.40	56.985	0.0001964	0.1687871	7.192
2-S	4.944	3.831	20.2	760	2.43	56.985	0.0001934	0.1662004	6.988
2-S	4.944	3.831	20.2	760	2.38	56.985	0.0001960	0.1684638	7.244
3-S	5.629	3.847	20.6	760	1.24	65.449	0.0125755	10.8209923	1046.857
3-S	5.629	3.848	20.6	760	1.22	65.449	0.0125566	10.8048029	1063.121
3-S	5.629	3.848	20.6	760	1.21	65.449	0.0125604	10.8080408	1072.578

Table (4-6) shows the core plugs gas permeability measured through the use of Permeameter which uses the nitrogen as the medium fluid calculated by darcy law.

TABLE-4.7 Conversion of apparent permeability (K_a to K_L)

SN	K_g	K_L
1-S	1.83	1.29
2-S	7.14	5.47
3-S	1060.85	1013.44

Table 4-7 shows the conversion of apparent permeability k_a measured by gas for an average pressure P_m to the true permeability k_L .

TABLE-4.8 Calculation of NaCl

Compound	Weight grams
NaCl	58.44
CaCl ₂ *2H ₂ O	147.01
MgCl ₂ *6H ₂ O	203.31
BaCl ₂ *2H ₂ O	244.27

Table 4-8 shows the weight of salts that used for the calculation of salt concentration which is found 6.16g of NaCl for 5 liters of distilled water.

TABLE-4.9 Calculation of brine saturant:

SN	Dry weight before sat.	Grain volume	Sat weight in air	Sat weight in saturant	Saturated pore vol	Corrected bulk vol	Saturation	Saturated porosity	Bulk volume
	G	Cc	G	G	cc	Cc	%	%	cc
1	124.08	46.78	139.29	76.61	15.18	15.76	96.31	24.27	62.54
2	114.05	43.12	127.46	70.64	13.38	13.57	98.60	23.60	56.69
3	121.92	45.99	138.90	76.04	16.94	16.73	101.29	27.01	62.72

Table 4-9 shows the core plugs brine saturation calculation by using ARCHMEDES method, after placing core plugs inside auto saturator machine.

TABLE-4.10 Absolute permeability measurement (SN1)

SN	flow rate (cc/hr)	Δp (psi)	Area (cm ²)	Length (cc)	Flowrate/area	$\Delta p /L$
1	1	2.2	11.728529	5.254	0.0852621813	0.4187286
	2	3			0.1705243627	0.5709935
	3	6			0.255786544	1.1419871

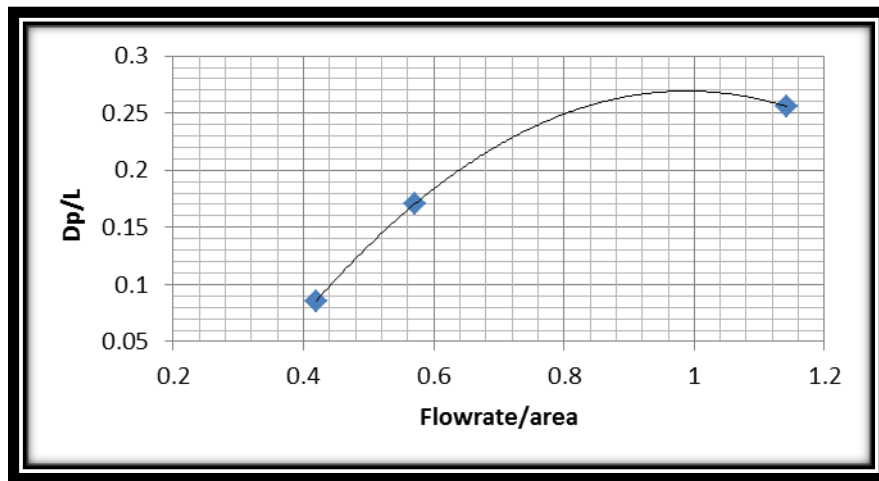


Fig. 4-2 Absolute permeability measurement (SN1)

Tables -4.10&Figure 4-2 shows the relationship of the differential pressure per length versus the flow rate per area, the deviation on curve indicates the non-darcy flow through the core plug (SN-01). The slope of the straight line section is permeability per the fluid viscosity (K/μ).

TABLE-4.11 Absolute permeability measurement (SN2)

SN	flow rate (cc/hr)	Δp (psi)	Area (cm ²)	Length (cc)	Flowrate/area	$\Delta p /L$
2	1	1.2	11.5211	4.94366667	0.0867972647	0.2427348
	2	1.4			0.1735945294	0.2831906
	3	1.6			0.2603917942	0.3236464

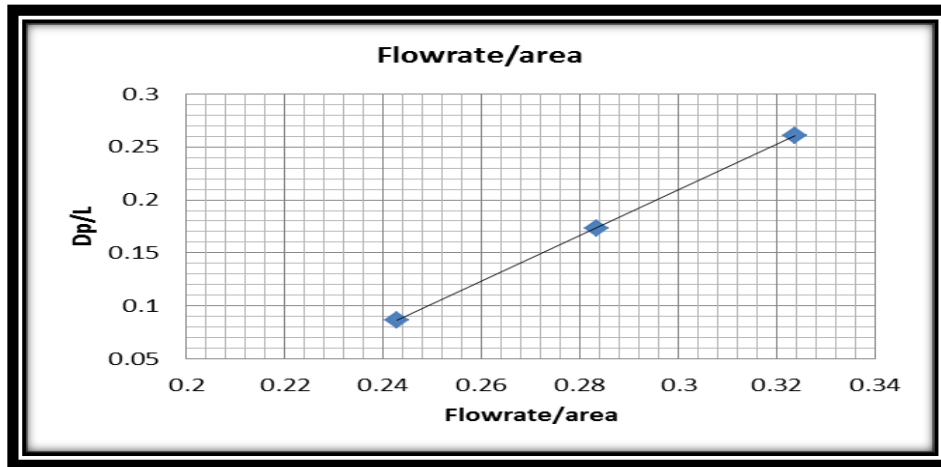


Fig. 4-3 Absolute permeability measurement (SN2)

Table- 4.11 & figure 4-3 shows the relationship of the differential pressure per length versus the flow rate per area, the straight line indicates the Darcy flow of flowing brine through core plug (SN-02) the slope of the line represents the permeability per the viscosity (K/μ). Unlike the flow through the core plugs SN-01.

TABLE-4.12 Absolute permeability measurement (SN3)

SN	flow rate (cc/hr)	Δp (psi)	Area (cm ²)	Length (cc)	Flowrate/area	$\Delta p /L$
3	10	1	11.620556	5.629	0.860544011	0.1776514
	20	1.5			1.721088021	0.2664772
	40	2.6			3.442176088	0.4618938

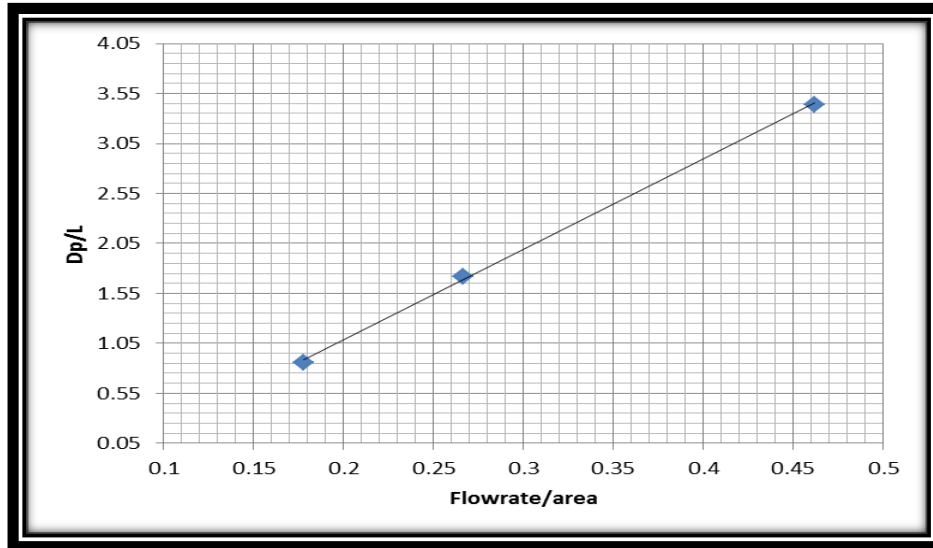


Fig. 4-4 Absolute permeability measurement (SN3)

Table- 4.12 & Figure 4-4 shows the relationship of the differential pressure per length versus the flow rate per area, the straight line indicates the Darcy flow of flowing brine through core plug (SN-03) the slope of the line represents the permeability per the viscosity (K/μ).

TABLE-4.13 Calculation of Initial and Residual Oil Saturation:

SN	PV	Water prod.	Oil prod	Sqz.	S_{wi}	$S_{wi\%}$	S_{oi}	$S_{oi\%}$	Sor
2	13.8	6	0.2	0.59	0.54579864	54.579864	0.454201	45.42014	0.254
3	19.4	9.9	0.45	0.59	0.47368421	47.368421	0.526316	52.63158	0.077

Table 4-13 shows the residual oil saturation for core plugs (SN-02 and SN-03), the residual oil saturation (25.5%) for SN-02 appears to be high with respect to the initial oil saturation (45.42%)

this is due to low rock permeability, resulting in large oil remaining inside the core pore space. And the residual oil saturation (7.7%) for SN-03 is quite low this is due to high permeability of core plug which result in good oil sweeping by water flood.

TABLE-4.14 Water flooding base case results (Core No-2)

TIME(min)	Q in(cc/min)	PV	oil pro	RE	T C°
0	3	0	0	0	25
10	3	30	0	0	25
20	3	60	0	0	25
30	3	90	0.01	0.00159152	25
40	3	120	0.02	0.003183041	25
50	3	150	0.04	0.006366082	25
60	3	180	0.05	0.007957602	25
70	3	210	0.07	0.011140643	25
80	3	240	0.08	0.012732163	25
430	3	1290	1.92	0.305571913	25
440	3	1320	2	0.318304076	25
450	3	1350	2.26	0.359683606	25
460	3	1380	2.35	0.374007289	25
470	3	1410	2.42	0.385147932	25
480	3	1440	2.58	0.410612258	25
490	3	1470	2.68	0.426527462	25
500	3	1500	2.73	0.434485064	25
510	3	1530	2.75	0.437668104	25
520	3	1560	2.76	0.439259625	25
530	3	1590	2.76	0.439259625	25

This table represents the data obtained from lab experiments without vibration as base case of water flooding

TABLE-4.15 Water flooding Results with Vibration, Core No-2

Time(min)	RE	PV	Total oil pro	oil pro	Freq(Hz)
540	0.439259625	1620	2.76	0	0.22
550	0.439259625	1650	2.76	0	0.22
560	0.439259625	1680	2.76	0	0.22
570	0.439259625	1710	2.76	0	0.22
680	0.439259625	2040	2.76	0	0.22
690	0.439259625	2070	2.76	0	0.22
700	0.472681553	2100	2.97	0.3	0.22
710	0.488596756	2130	3.07	0.4	2.00
720	0.488596756	2160	3.07	0.4	2.00
730	0.488596756	2190	3.07	0.4	2.00
740	0.488596756	2220	3.07	0.4	2.00
750	0.488596756	2250	3.07	0.4	3.83
760	0.488596756	2280	3.07	0.4	3.83
770	0.488596756	2310	3.07	0.4	3.83
780	0.488596756	2340	3.07	0.4	3.83

Table 4-15 shows the increment in the recovery factor obtained due to application seismic stimulation.

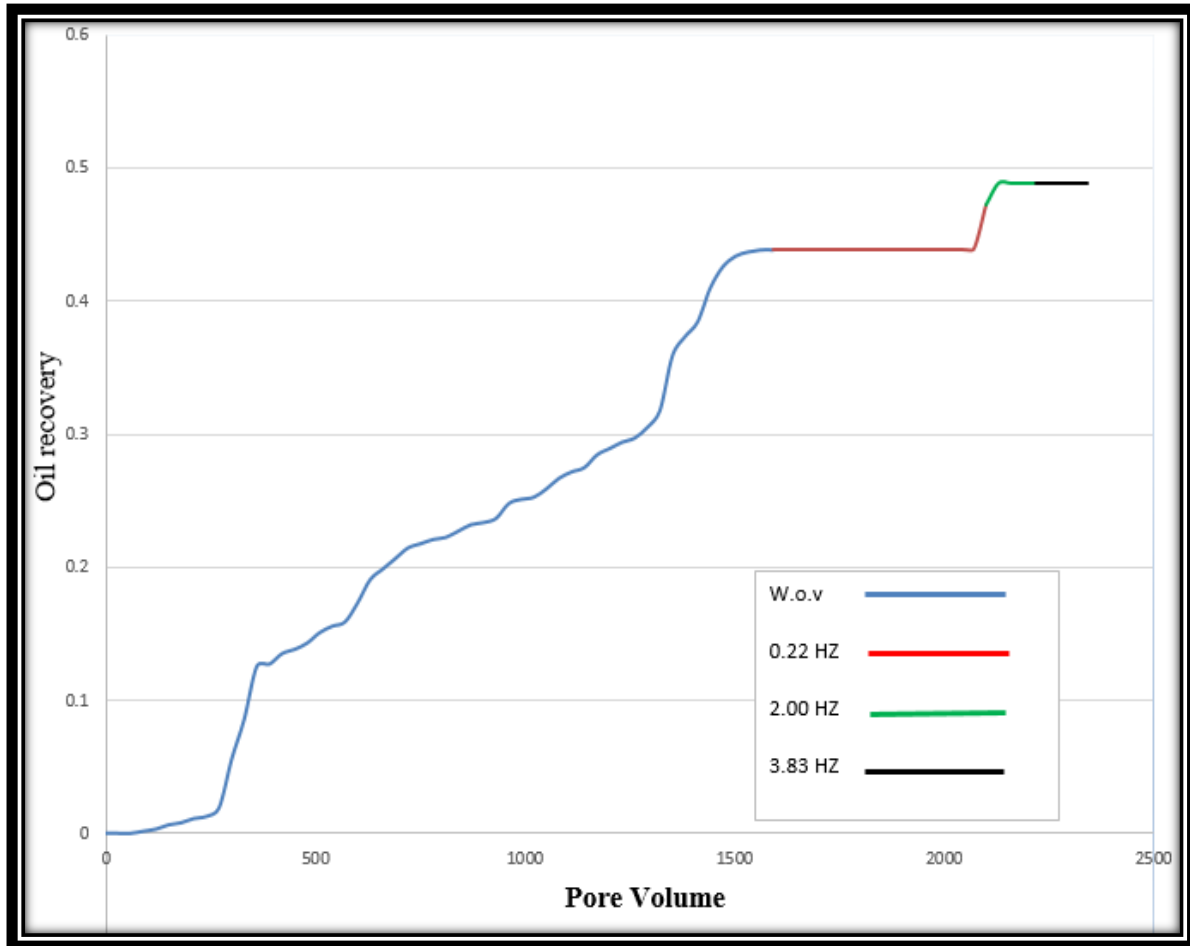


Fig. 4-5 Plot of oil recovery vs. pore volume injected (SN2)

- The decline in the curve (flooding without vibration) indicates that there is no more oil can be recovered.
- The straight line indicates that the vibration effect does not take place yet.
- The upward movement indicates that the vibration effect has taken place.
- The straight line in the end of the curve means there is no more oil can be recovered by vibration stimulation.

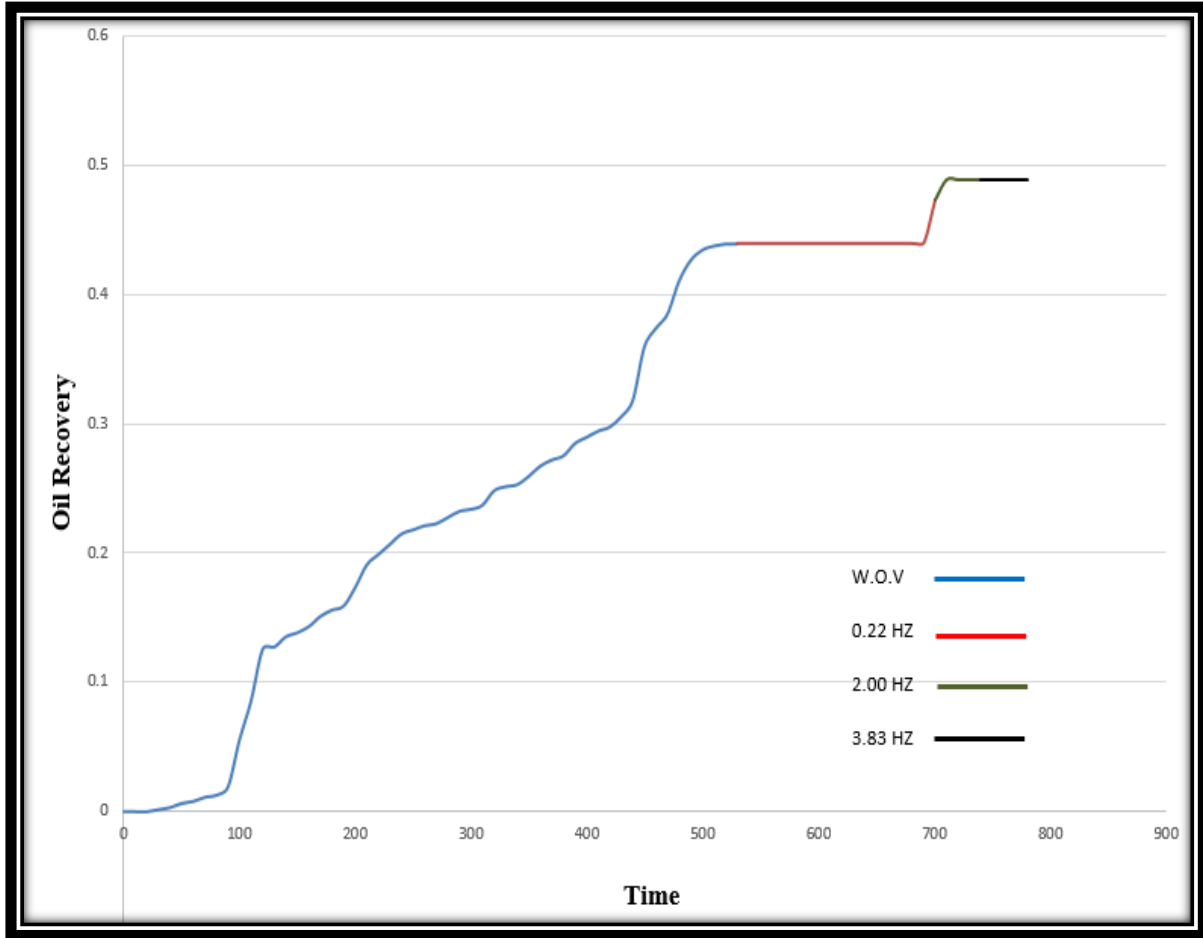


Fig. 4-6 Plot of oil recovery (cc) vs. time (min)

The figure shows the steady increment on oil recovery as function of core exposure time to vibration stimulation.

TABLE-4.16Water flooding base case results Core No-3

TIME _(min)	Q in (cc/min)	PV	OIL pro	RE	T C°
0	20	0	0	0	23
10	20	200	0	0	23
20	20	400	0.3	0.029382	23
30	20	600	0.9	0.088145	23
40	20	800	1.21	0.118505	23
50	20	1000	1.87	0.183145	23
60	20	1200	2.26	0.221341	23
70	20	1400	2.6	0.25464	23
80	20	1600	2.89	0.283042	23
190	20	3800	7.11	0.696342	23
200	20	4000	7.31	0.71593	23
210	20	4200	7.76	0.760002	23
220	20	4400	8.13	0.796239	23
230	20	4600	8.45	0.827579	23
240	20	4800	8.66	0.848147	23
250	20	5000	8.7	0.852064	23
260	20	5200	8.71	0.853043	23
270	20	5400	8.71	0.853043	23
280	20	5600	8.71	0.853043	23

Table 4-16 shows the base case data of oil recovery obtained by the water flooding with no vibration as appears high oil recovered by water flooding this due to high permeability of core plugs.

TABLE-4.17 Water flooding Results With Vibration, Core No-3

TIME _(min)	Q _{in(cc/min)}	PV	Oil Pro	Total Oil _(cc)	Freq (HZ)	RE	T C°
290	20	5800	0	8.71	0.24	0.853043436	23
300	20	6000	0	8.71	0.24	0.853043436	23
310	20	6200	0.1	8.81	0.24	0.862837275	23
320	20	6400	0.2	8.81	0.24	0.862837275	23
330	20	6600	0.3	8.91	0.24	0.872631115	23
340	20	6800	0.3	8.91	0.24	0.872631115	23
350	20	7000	0.3	8.91	2.33	0.872631115	25
360	20	7200	0.4	9.11	2.33	0.892218794	25
370	20	7400	0.4	9.11	2.33	0.892218794	25
380	20	7600	0.4	9.11	2.33	0.892218794	25
390	20	7800	0.5	9.21	2.33	0.902012634	25
400	20	8000	0.5	9.21	2.33	0.902012634	25
410	20	8200	0.5	9.21	3.43	0.902012634	25
420	20	8400	0.5	9.21	3.43	0.902012634	25
430	20	8600	0.5	9.21	3.43	0.902012634	25
440	20	8800	0.5	9.21	3.43	0.902012634	25
450	20	9000	0.5	9.21	3.43	0.902012634	25
460	20	9200	0.5	9.21	3.43	0.902012634	25

Table 4-17 shows the recovered oil by vibration while flooding, the oil recovered has increased due to stimulation and the high oil recovery percentage is a result of high core permeability.

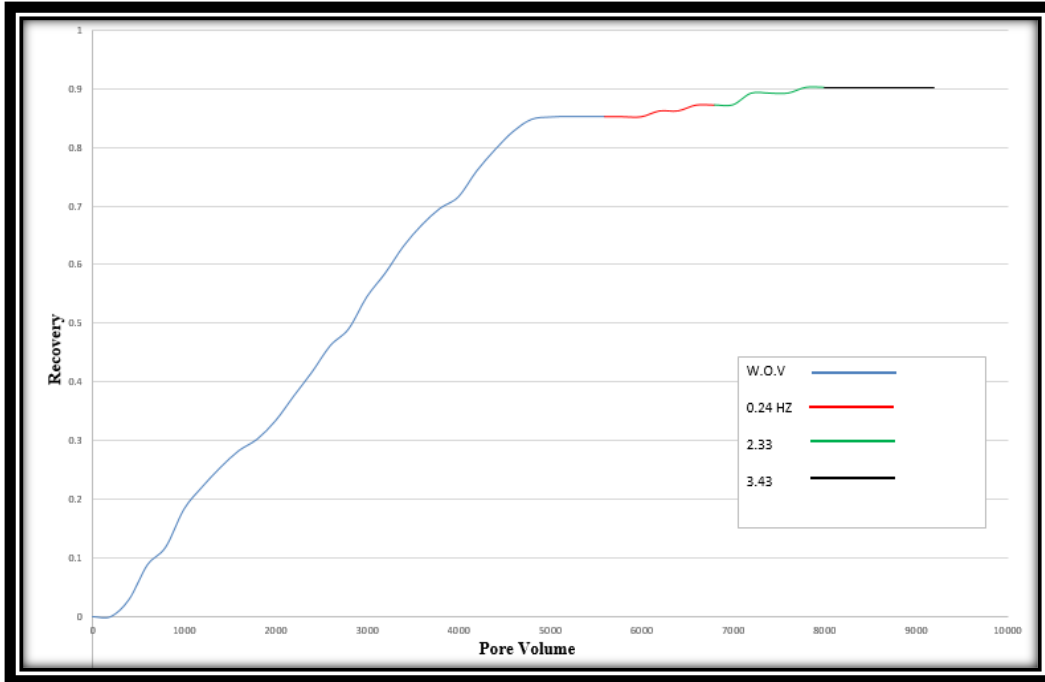


Fig. 4-7Plot of Oil Recovery (cc) vs. Pore Volume Injected (SN3)

The figure indicates the steady increment in oil recovery after exposing the core plugs to vibration also the change of vibration intensity has shown the ability in increasing the recovery.

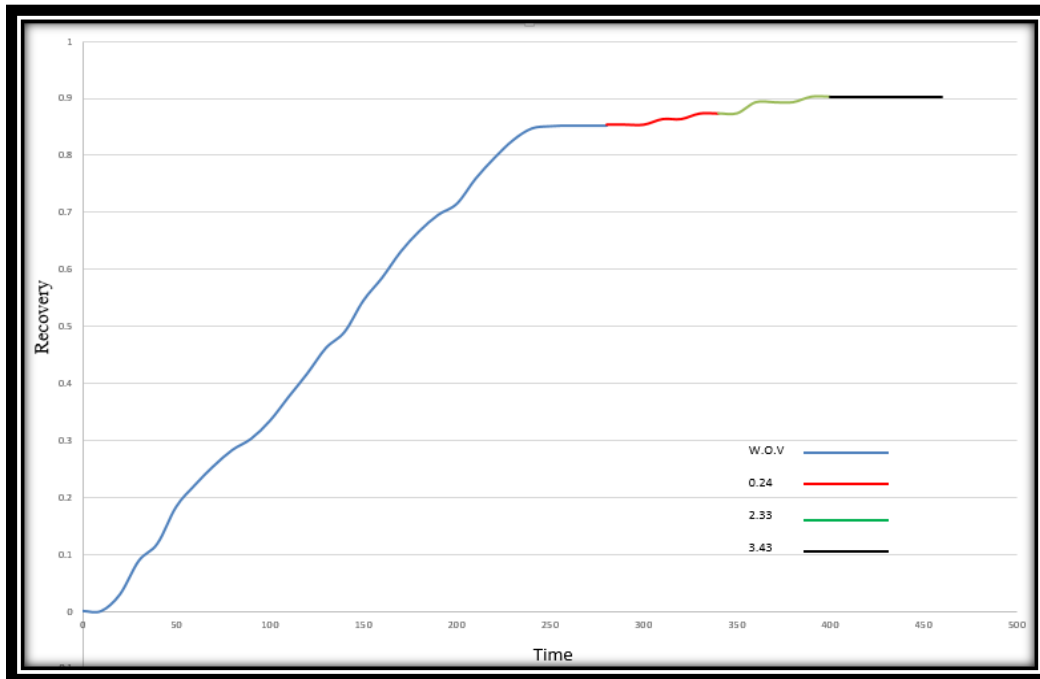


Fig. 4-8 Plot of Oil Recovery (cc) vs. Time (min)

Table-4.18 Relation between S_{or} before & after Seismic Simulation

SN	Previous S_{or}	RF%	Recent S_{or}	Recent RF%	Recovered oil %
1	0.254	43.925	0.2317	48.856	11.41
2	0.077	85.304	0.0515	90.201	33.47

CHAPTER 5

Conclusion And Recommendations

Chapter 5

5.1 Conclusion:

Based on this study ISS is expected to be an excellent EOR method for residual oil extraction. As a result of the study increment of oil recovery was observed when vibration applied to the core plugs, also it was observed that vibration intensity and vibration exposing time have strong effect for oil mobilization from pore space, in addition to this it was observed that the formation permeability influence the oil recovery which in turns leads to poor or good oil displacement.

-Samples selecting for testing are from one layer, represent different rock properties.

Type 1:

Of very poor quality reservoir rock (with average $k_a=1.834\text{md}$, $\phi = 24.17$, depth= 1430.04m , volume= 61.626 cm^3)

Type 2:

Of near tight reservoir rock (with average $k_a =7.141\text{md}$, $\phi =24.29$, depth= 1432.34m volume= 56.956 cm^3)

Type 3:

Of high quality reservoir rock (with average $k_a=1060.852\text{md}$, $\phi =29.62$, depth= 1434.00m volume= 65.416 cm^3).

1. Sample 2: initial water saturate S_{wi} is 54.579864 (%PV) from relative Permeability while S_{or} is Averaging 25.4 (% PV) and initial oil saturation S_{oi} of 45.42014 (%PV).
2. Sample 3: initial water saturate S_{wi} is 47.368421 (%PV) from relative Permeability while S_{or} is Averaging 7.7 (% PV) and initial oil saturation S_{oi} of 52.63158 (%PV).
3. Sample 2: the maximum oil recovery obtained without vibration was 43.92% , and the maximum oil recovery obtained with vibration was 48.85% , the increment is 4.9% and oil residual saturation decreased from 25.4% to 23.17% .
4. Sample 3: the maximum oil recovered without vibration was 85.3% , and the maximum oil recovered with vibration was 90.2% the increment in oil recovery is 4.9% and oil residual saturation decreased from 7.7% to 5.15% .

5.2 Recommendations:

The experiment has approved that oil recovery could be increased by significant value through application of seismic simulation, despite of that and for optimum application of the method more studies should be conducted and should include:-

- Investigation of vibration effects on oil and water relative permeability.
- Investigation of vibration effects on oil recover at different reservoir conditions (i.e. pressure and temperature).
- Study the effect of vibration on rock Capillary pressure and pore throats.
- Further studies on core plugs of various levels of oil and water saturation in order to determine the optimum recovery and optimum time to start vibration.
- Should study the vibration effectiveness on homogeneous and heterogeneous formations
- To determine the effectiveness of the seismic stimulation application in different rocks porous mediums (i.e. sandstone, limestone and carbonates).

References:-

- 1) Mihailo Jankov “Two phase flow in porous medium with and without seismic stimulation” University of Oslo, Norway March 2010
- 2) Steven R. Pride, Flekkoy and Olave “Seismic Stimulation for Enhanced Oil Recovery” January 2008.
- 3) Robert Wester Mark “Enhanced Oil recovery with Downhole Vibration Stimulation” November 2003.
- 4) Peter M. Roberts', Ernest L. Majer, Wei-Cheng Lo, Garrison Sposito, and Thomas M. Daley “An integrated approach to seismic stimulation of oil reservoir” august 2002.
- 5) O. Torsater M. Abtahi ‘Experimental Reservoir Engineering Laboratory Work Book’ Norwegian University August 2000.